

HOSTED BY



ELSEVIER

Available online at [www.sciencedirect.com](http://www.sciencedirect.com)**ScienceDirect**journal homepage: <http://ees.elsevier.com/ejbias/default.asp>**Full Length Article**

# Facies analysis, glauconite distribution and sequence stratigraphy of the middle Eocene Qarara Formation, El-Minya area, Egypt



Omar A. Hegab <sup>a</sup>, Mohamed A. Serry <sup>b</sup>, Tarek I. Anan <sup>a,\*</sup>,  
Ahmed G. Abd El-Wahed <sup>a</sup>

<sup>a</sup> Department of Geology, Faculty of Science, Mansoura University, Mansoura, Egypt

<sup>b</sup> Ceramic Department, National Research Center, 12622-Dokki, Cairo, Egypt

**ARTICLE INFO****Article history:**

Received 1 August 2015

Received in revised form 2

September 2015

Accepted 8 September 2015

Available online 23 October 2015

**Keywords:**

Sequence stratigraphy

Middle Eocene

Qarara Formation

Glauconite

Egypt

**ABSTRACT**

The Qarara Formation consists mainly of shale at the base and overlain by limestone at the top. The formation is Middle Eocene (Lutetian) in age. Three sections located at the eastern bank of the Nile River in El-Minya Province have been measured, described, and sampled. These sections from north to south are: Gebel Qarara, El-Sheikh Fadl, and Gebel El-Ahmar.

The main microfacies identified in the studied sections are: silty claystone, silty shale, fossiliferous glauconite, glauconitic (green) sand, glauconitic fossiliferous ironstone, glauconitic bioclastic wacke-packstone, glauconitic bioclastic lime-mudstone-wackestone. These microfacies have been deposited in shallow open marine environment.

Collectively the studied rocks contain two principal facies: lower argillaceous facies and upper carbonate facies that separated by glauconitic fossiliferous ironstone bed. The lower argillaceous part represents highstand systems tract (HST), whereas the upper carbonate part represents transgressive systems tract (TST). The glauconitic fossiliferous ironstone bed is recognized as a sequence boundary (SB).

© 2015 Mansoura University. Production and hosting by Elsevier B.V. This is an open access article under the CC BY-NC-ND license (<http://creativecommons.org/licenses/by-nc-nd/4.0/>).

---

## 1. Introduction

The study area includes five mappable Eocene rock units: the Beni Suef Formation, the Samalut Formation, the Maghagha Formation, the Qarara Formation, and the El Fashn Formation. These five formations are Middle Eocene in age [1–3].

The Eocene succession exposed in the east bank of the Nile River between Maghagha and El-Fashn is similar in gross lithologic characters to the succession developed in the area south of Fayum [4]. In the Fayum area, the formation names Maghagha, Qarara, and El-Fashn are replaced by the Muweilih, Midawara, Sath el Hadid, and Gharaq formations by Iskander [5].

\* Corresponding author. Tel.: +20 00201027393868.

E-mail address: [atarek@mans.edu.eg](mailto:atarek@mans.edu.eg) (T.I. Anan).

<http://dx.doi.org/10.1016/j.ejbias.2015.09.002>

2314-808X/© 2015 Mansoura University. Production and hosting by Elsevier B.V. This is an open access article under the CC BY-NC-ND license (<http://creativecommons.org/licenses/by-nc-nd/4.0/>).

The present studied rock units belong to the Qarara Formation which was described by Bishay [3] and Omara et al. [6] on the basis of its *Nummulites* sp. content. The Qarara Formation is Late Lutetian in age by Cronin and Khalifa [7] due to the presence of smaller and larger foraminifera. The present study focuses on facies development, distribution of glauconite, and sequence architecture of the Middle Eocene Qarara Formation.

## 2. Material and methods

Three outcrop locations were sampled, measured, and examined in detail (Fig. 1). From north to south, these sections are: Gebel Qarara section (Lat.  $28^{\circ} 38' 49.6''$  N, Long.  $30^{\circ} 52' 40.6''$  E), El-Sheikh Fadl section (Lat.  $28^{\circ} 30' 48.1''$  N, Long.  $30^{\circ} 54' 40.3''$  E), and Gebel El Ahmar section (Lat.  $28^{\circ} 28' 22.6''$  N, Long.  $30^{\circ} 57' 20.7''$  E). Sixteen shale samples and seven carbonate ones were collected to represent the Qarara Formation. The collected samples were subjected to various analyses in the laboratory. These include general analyses of sediment texture, petrography, and X-ray Diffraction analysis. Twenty three thin sections were prepared and described under the polarizing

microscope. Limestone microfacies were described following the classification of Dunham [9].

Separation of clay fraction and preparation of samples for XRD analysis are normal routine work. Three oriented mounts were prepared for each sample. These typically include: (1) air-dried sample, (2) heating to  $550^{\circ}\text{C}$ , for kaolinite destruction and dehydration of smectite which potentially hide chlorite peaks, and (3) treatment by ethylene glycol in order to reveal expandable clay minerals [10].

## 3. Stratigraphy

The Middle Eocene rocks are developed at the east bank of the Nile River between Beni Suef and El-Minya Governorates. This area displays a complex variation in lithology and hence has been given formational names as listed in Table 1.

The term Qarara Formation was used by Bishay [3] for the sequence of Gebel Qarara that forms the northern boundary of the Maghagha district. The Qarara Formation is Middle Eocene (Lutetian) in age and is composed of grey to green shale at its base (Fig. 2A) and grading upward to marl and limestone at the top (Fig. 2B).

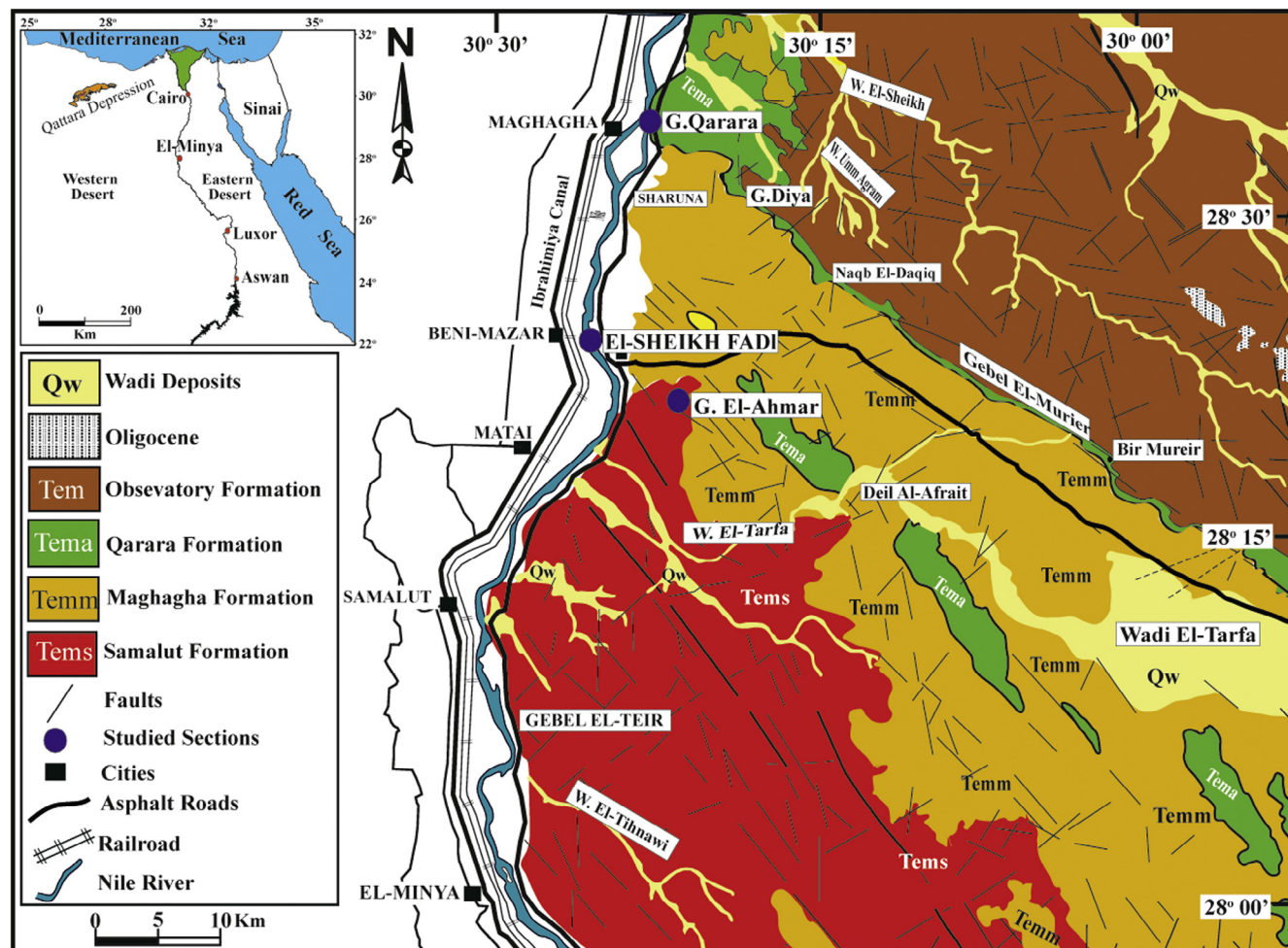
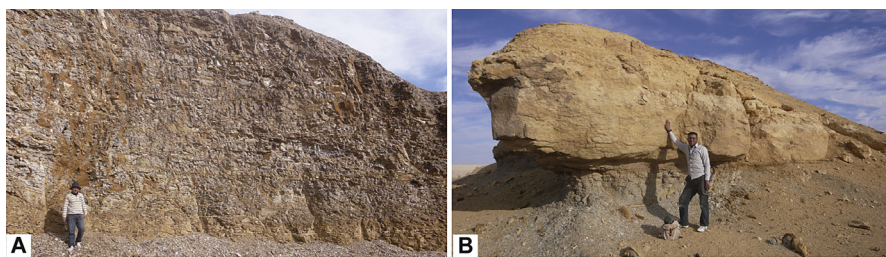


Fig. 1 – Geologic map and location of the studied area [8].

**Table 1 – Middle Eocene formations and their formal units [2–4,34].**

Location	Nile Valley		Fayum area	Present work
Author	Bishay (1961, 1966) [2,3]	Bassiouni et al. (1977) [34]	Strougo (1986) [4]	
Formation	Beni Suef Formation	Mokattam Formation	Upper Building stone Member	Midawara Formation
	El-Fashn Formation		Beni Suef Member	Beni Suef Formation
	<b>Qarara Formation</b>		Gizehensis Member	El-Fashn Formation
	Maghagha Formation		Lower Building stone Member	<b>Qarara Formation</b>
	Samalut Formation		Samalut Member	Maghagha Formation
				Samalut Formation



**Fig. 2 – Field photographs showing: (A) the lower part of the Qarara Formation which is composed mainly of grey to green shale, person for scale is 1.7 m; (B) the upper carbonate part of the Qarara Formation, person for scale is 1.7 m.**

The Qarara Formation overlies the Maghagha Formation, underlies El-Fashn Formation, and extends to Gebel Merier and Wadi Tarfa in the Egyptian Eastern Desert. Its fossil content comprises *Nummulites gizehensis* and *Globorotalia centralis* [3]. In outcrop, this formation is represented by mixed shale-limestone successions (Fig. 3).

## 4. Results and discussion

### 4.1. Particle size distribution

The study of particle sizes in the clayey samples was carried out using the pipette method adopted by Folk [11]. The results are summarized in Table 2 and illustrated in the triangular diagram of Picard [12] (Fig. 4). According to the classification of Picard [12], the fine sediments of Gebel El-Ahmar samples fall into clay and silty clay categories, the Sheikh Fadl samples are classified as clay, silty clay, sandy clay and clayey mud categories, whereas the Gebel Qarara samples fall into clay and silty clay categories. Therefore, all the studied clay and silty clay categories could be considered as fissile claystone or shale [13]. The sand fractions of the sandy clay of El-Sheikh Fadl contain high amounts of glauconite pellets, and they are considered as glauconitic sandy clays. The vertical grain size distributions through the studied sections are illustrated in Figs. 5–7.

### 4.2. Facies analysis

#### 4.2.1. Mudrocks microfacies

4.2.1.1. Silty claystone. Clay fraction in the silty claystone microfacies varies between 71.92% and 99.13% with an average of 84.23%. X-ray diffraction analysis indicates that the common minerals are smectite and kaolinite (Fig. 8a). The main components of this microfacies are quartz and feldspars that are scattered in a clay matrix. Quartz and feldspar grains are very angular to subangular (Fig. 9A). Claystones are internally homogeneous and contain no visible bioturbation. Pyrite is ubiquitous in claystone microfacies and occurs as disseminated anhedral to euhedral crystals and as irregular patches (Fig. 9B).

4.2.1.2. Silty shale. In silty shale microfacies, clay fraction ranges from 52.23 to 94.56% with an average of 77.88%. Quartz and feldspars vary between 5.45 and 15.14% with an average of 10.29% and are concentrated into discrete quartz laminae (Fig. 9C), while the reminders are abundant in a clay matrix. Most quartz grains are subangular to angular but a few are subrounded (Fig. 9D).

Most clay particles are white (Fig. 9E), whereas some are green. X-ray diffraction indicates that they compose mainly of smectite and kaolinite with traces of illite (Fig. 8b). In quartz-poor silty shale microfacies, clays are uniformly elongate parallel to laminae (Fig. 9F). Fissures in the silty shale microfacies are either later infilled with gypsum (Fig. 10A) or hematite (Fig. 10B).

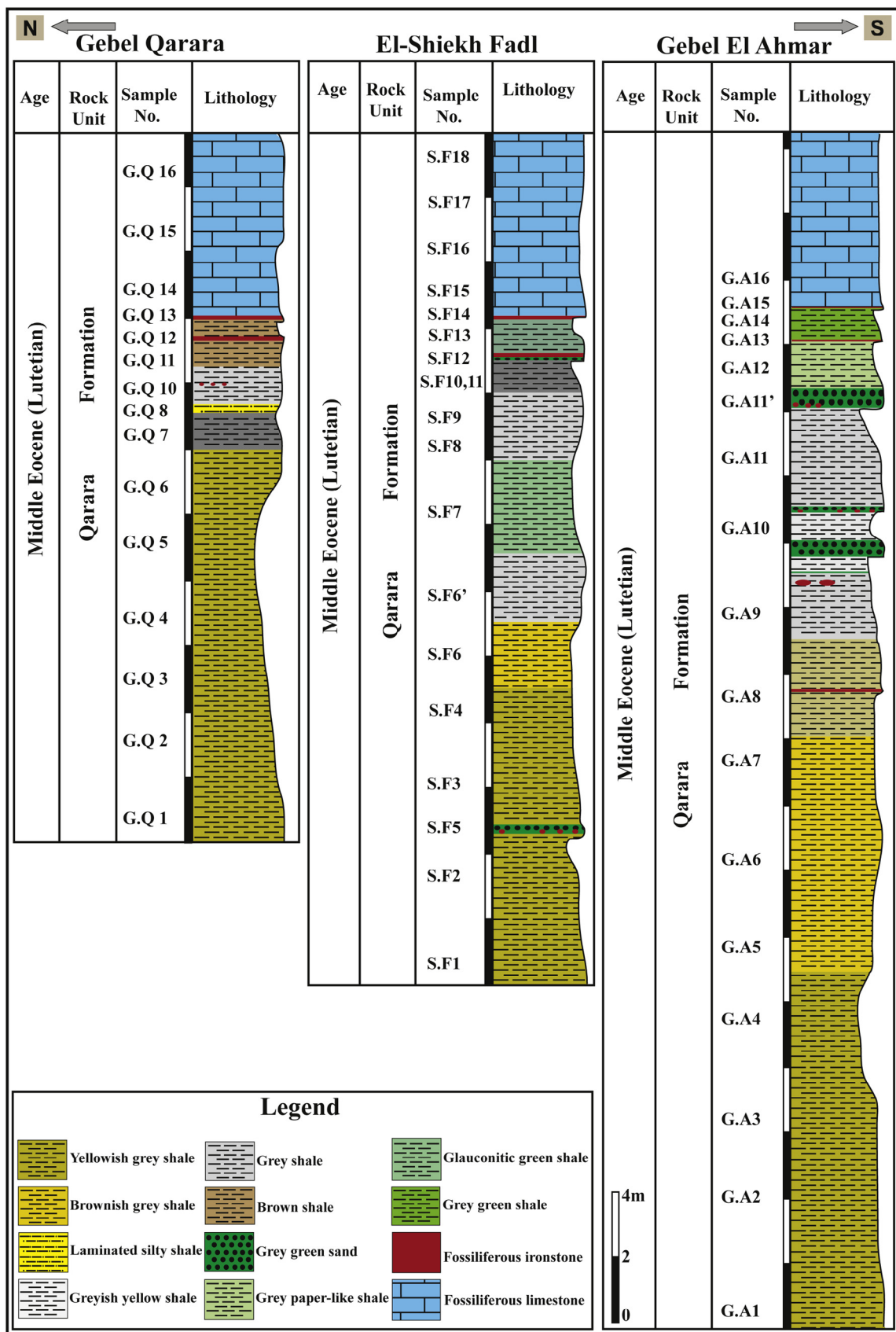


Fig. 3 – Lithostratigraphy of the three studied sections: Gebel Qarara, El-Sheikh Fadl, and Gebel El-Ahmar.

**Table 2 – Grain size distribution for selected clay samples from the Qarara Formation.**

Location	Sample no.	Clay size classes				
		>5Φ	5 Φ	6 Φ	7 Φ	8 Φ
Gebel Qarara	G.Q01	0.24	0.08	5.93	3.17	5.93
	G.Q06	1.68	2.07	0.79	1.30	5.98
	G.Q08	0.35	10.90	5.39	2.87	8.58
	G.Q12	3.25	23.97	11.49	2.61	6.44
El-Sheikh Fadl	S.F01	0.11	4.29	6.82	4.13	8.20
	S.F06	27.64	11.81	2.55	9.69	9.35
	S.F07	33.58	1.42	3.54	2.12	4.80
	S.F08	1.62	5.29	1.02	2.01	2.28
	S.F10	0.57	5.49	6.96	4.79	12.36
Gebel El-Ahmar	S.F13	10.60	3.61	0.33	0.37	6.07
	G.A02	-	4.57	5.63	1.72	3.22
	G.A06	0.24	0.15	0.53	1.45	3.08
	G.A07	1.56	3.63	1.43	1.31	1.33
	G.A09	0.25	5.63	4.45	4.71	2.80
	G.A10	5.39	26.96	0.69	4.85	3.57
	G.A14	5.28	7.70	9.17	3.59	5.37

Clay pellets are scattered within silty shale microfacies with long axes almost parallel to lamination (Fig. 10C).

Two types of lamination are determined in silty shale microfacies: quartz laminae and clay laminae (Fig. 10D). Quartz laminae are both continuous and discontinuous in approximately equal amounts. Clay laminae on the other hand vary in thickness.

Interpretation: Shale and claystone in the studied rock unit represent relatively quiet water deposition in a distal setting, likely dominated by suspension fall-out, although some bed load processes and weak currents may have been involved [14].

#### 4.2.2. Glauconite microfacies

**4.2.2.1. Fossiliferous glauconite.** This microfacies is composed mainly of tightly spaced angular to subangular silt-sized

quartz grains intermixed with rounded to subrounded, slightly oxidized glauconite pellets (Fig. 10E). Both quartz and glauconite grains are floated in a clay matrix. Large shell fragments are scattered in a fine clay matrix (Fig. 10F).

Interpretation: The presence of glauconite is a good indicator of shallow marine settings [15,16]. In addition, the presence of bivalve fragments is an indication of low energy open shallow marine shelf environment [17].

**4.2.2.2. Glauconitic (green) sand.** This microfacies is composed of sand-sized, subrounded, yellow to pale green glauconite grains, in addition to quartz grains with a limited distribution. Glauconite and quartz are embedded in a glauconitic clay matrix (Fig. 11A). Most of the examined sections of this microfacies are well sorted and few are poorly sorted (Fig. 11B). The majority of the encountered glauconite grains are fractured, whereas some smooth grains are recorded (Fig. 11C).

Interpretation: Glauconite forms exclusively in marine environments. McRae [18] stated that the accumulation of glauconite in large quantities indicates a low rate of sedimentation with normal marine salinity and weakly reducing environments. Because glauconite is slow to form, it is usually common with a transgression of relative sea level [19].

**4.2.2.3. Glauconitic fossiliferous ironstone.** This microfacies consists of well rounded, well sorted, silt-sized glauconitic grains. Echinoderms, miliolid foraminifera, large gastropods, ostracods, and bryozoans are floated in a hematitic cement (Fig. 11D, E). Glauconite grains exhibit different degree of diagenetic alteration which resulted in the progressive development of iron oxides. Such alteration proceeds either from outer rim of the glauconite grains to the center or from inside to outside, but from outside is the prominent alteration. Fossil moulds are partially or completely replaced by iron oxides (Fig. 11F).

#### 4.2.3. Carbonate microfacies

These microfacies are almost recorded in the uppermost parts of the studied sections just overlying the glauconitic fossiliferous ironstone bed. They are glauconitic in both Gebel El-Ahmar

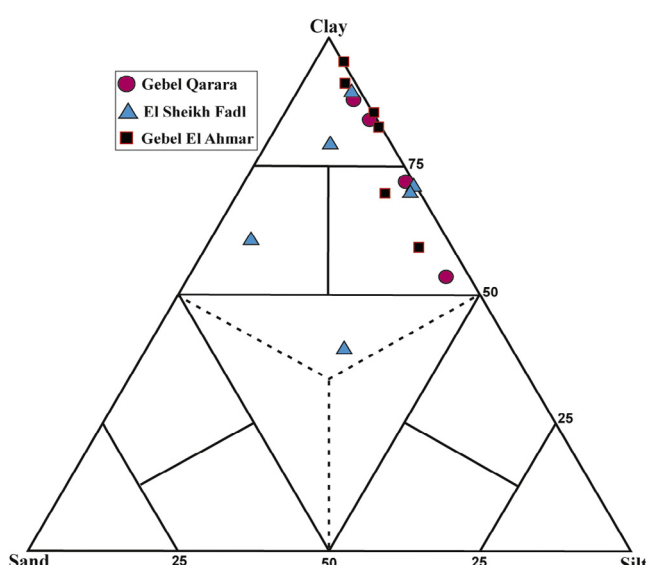


**Fig. 4 – Particle size distribution of the Qarara shale samples (after Picard, 1971). G.A.: Gebel Qarara section, S.F.: El-Sheikh Fadl section, and G.Q.: Gebel El Ahmar section.**

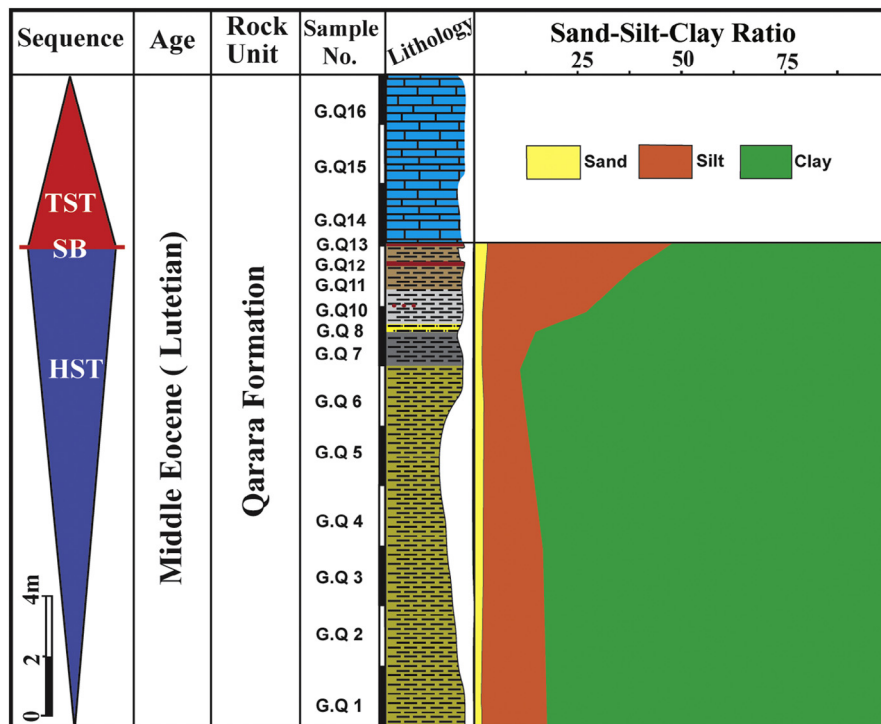


Fig. 5 – Vertical distribution of sand-silt-clay and sequence stratigraphy of the Qarara Formation in Gebel Qarara section. For legend see Fig. 3.

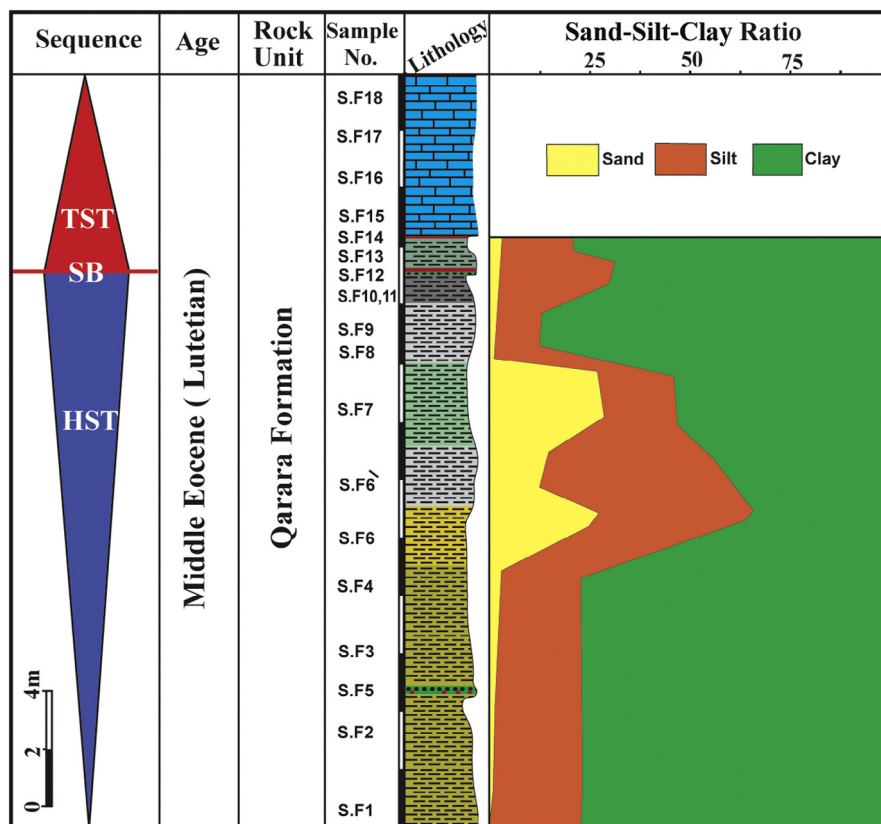


Fig. 6 – Vertical distribution of sand-silt-clay and sequence stratigraphy of the Qarara Formation in El-Sheikh Fadl section. For legend see Fig. 3.

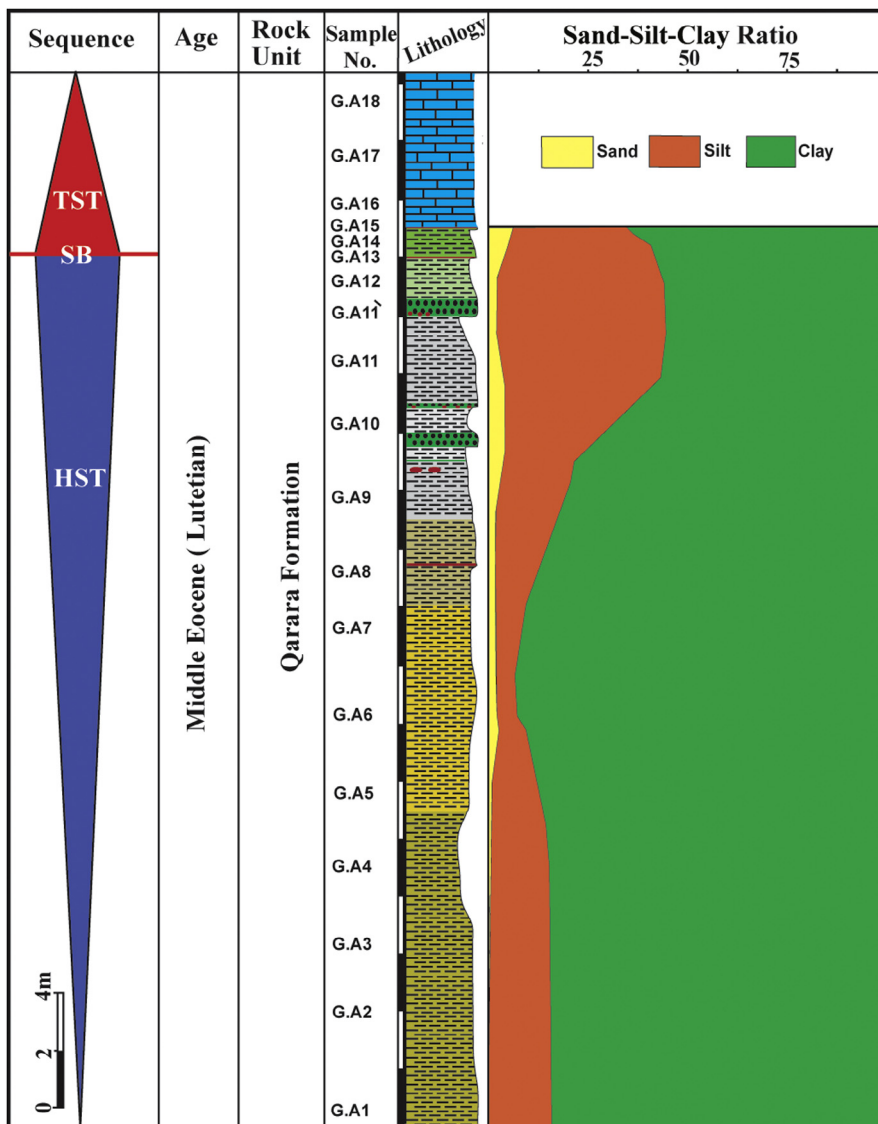


Fig. 7 – Vertical distribution of sand-silt-clay and sequence stratigraphy of the Qarara Formation in Gebel El-Ahmar section. For legend see Fig. 3.

and Gebel Qarara sections. Carbonate units are represented by two microfacies: glauconitic bioclastic wacke-packstone and glauconitic bioclastic lime-mudstone-wackestone.

**4.2.3.1. Glauconitic bioclastic wacke-packstone.** This microfacies is dominated by nummilitic shells (Fig. 12A) with some miliolid foraminifera, echinoderm fragments, bryozoans of fenestral types and ostracods and well sorted, rounded glauconitic grains. The microfacies is characterized by large-sized nummilites with radial hyaline walls. Nummilites also show a pronounced extinction bands (Fig. 12B) that resulted from radial calcite crystals. The excellent preservation of these nummilitic shells (Fig. 12C) indicates that they originally comprised low Mg-calcite [20]. The allochemical components are embedded in a fine-grained micrite matrix. Some cavities show geopetal-like structure

(Fig. 12D) where large mosaic calcite crystals occupy parts of the cavity, and the rest is occupied by the original micrite infill.

**Interpretation:** This microfacies is similar to SMF 5 and FZ 6 [21,22]. The microfacies is deposited in an agitated shoal environment where large shell fragments were abraded by wave action.

**4.2.3.2. Glauconitic bioclastic lime-mudstone-wackestone.** This microfacies is dominated by bryozoans, echinoderm spines, nummilites, miliolid foraminifera that embedded in a micrite matrix (Fig. 12E). Fine sand-sized quartz grains and glauconite pellets are also encountered. Nummilitic tests are fewer in number and smaller in size (Fig. 12F) than the previous microfacies. The recrystallization of the dull micrite matrix into

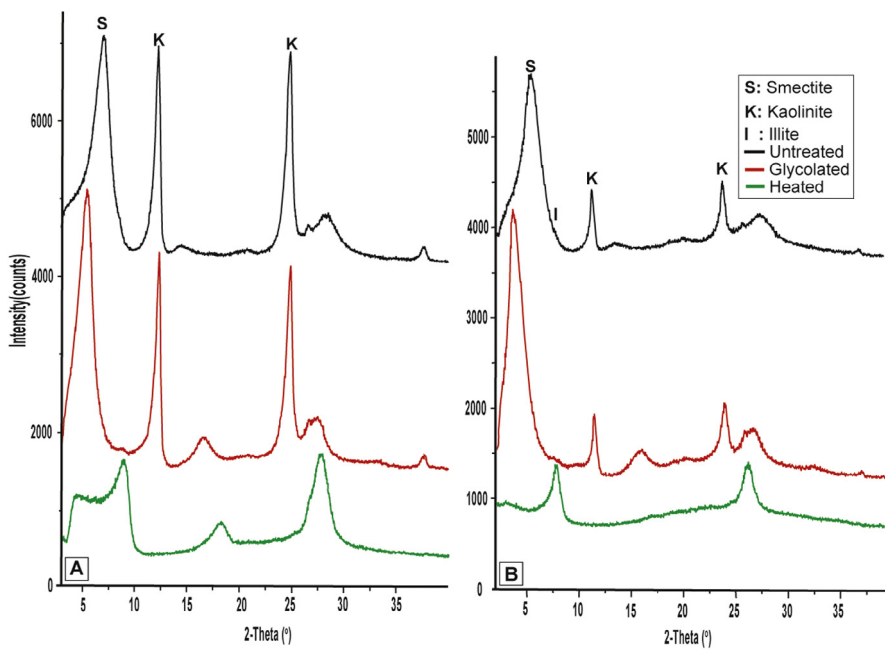


**Fig. 8 – Representative XRD tracing of clay fraction of (A) silty claystone microfacies and (B) silty shale microfacies.**

microspar with high birefringence is the main diagenetic process that affected this microfacies.

**Interpretation:** Low diversity fauna that composed of bivalves are commonly associated with muddy, shallow lagoon environments [17]. This microfacies is equivalent to SMF 9 and FZ 7 [21,22] that suggests deposition in shallow lagoon settings.

#### 4.3. Depositional environments

Shale and claystone in the studied Qarara Formation were deposited in a quiet water environment. The presence of glauconite represents a condensed setting in an overall calm environment [23,24]. The carbonate microfacies are deposited in inner ramp settings because of the presence of larger foraminifera and bivalves [22].

### 5. Sequence stratigraphy

The application of sequence stratigraphy has led to improve our understanding of how stratigraphic units, facies tracts, and depositional elements relate to each other in time and space [25]. Galloway [26] defined depositional systems as three-dimensional assemblages of process-related facies that record major paleogeomorphic elements. The linkage of contemporaneous depositional systems is forming the subdivision of a sequence [27].

#### 5.1. Sequence boundaries and systems tracts

In the studied sections, the recorded sequence boundary is characterized by local subaerial exposure. This sequence boundary has been recorded in the glauconitic fossiliferous ironstone bed between shale and limestone facies (Fig. 13A, B). Glauconite in this bed was subjected to extensive oxidation during subaerial exposure, so that colour of the glauconite and the whole bed changed to brownish red (Fig. 13). Some glauconite grains show oxidation from the outer rim to the central part of the grain, whereas others show reverse regime (Fig. 11E, F).

Lowstand systems tract (LST) is not recorded in the studied succession due to absence of coarse-grained sediments and minor subaerial unconformity. Highstand systems tract (HST) is generally characterized by varicoloured shale beds (Fig. 12). These shale beds are deposited in shallow to open marine environment. Relative sea level rises are recognized from the microfacies that comprise the transgressive systems tract (TST). These microfacies are dominated by wackestone-packstone microfacies which overlie the recorded sequence boundary.

#### 5.2. Glauconite in sequence stratigraphy

Glauconite formation and maturation require prolonged residence at or near the sediment–water interface and hence is a reliable indicator of low sedimentation rate [23]. Thus, occurrence

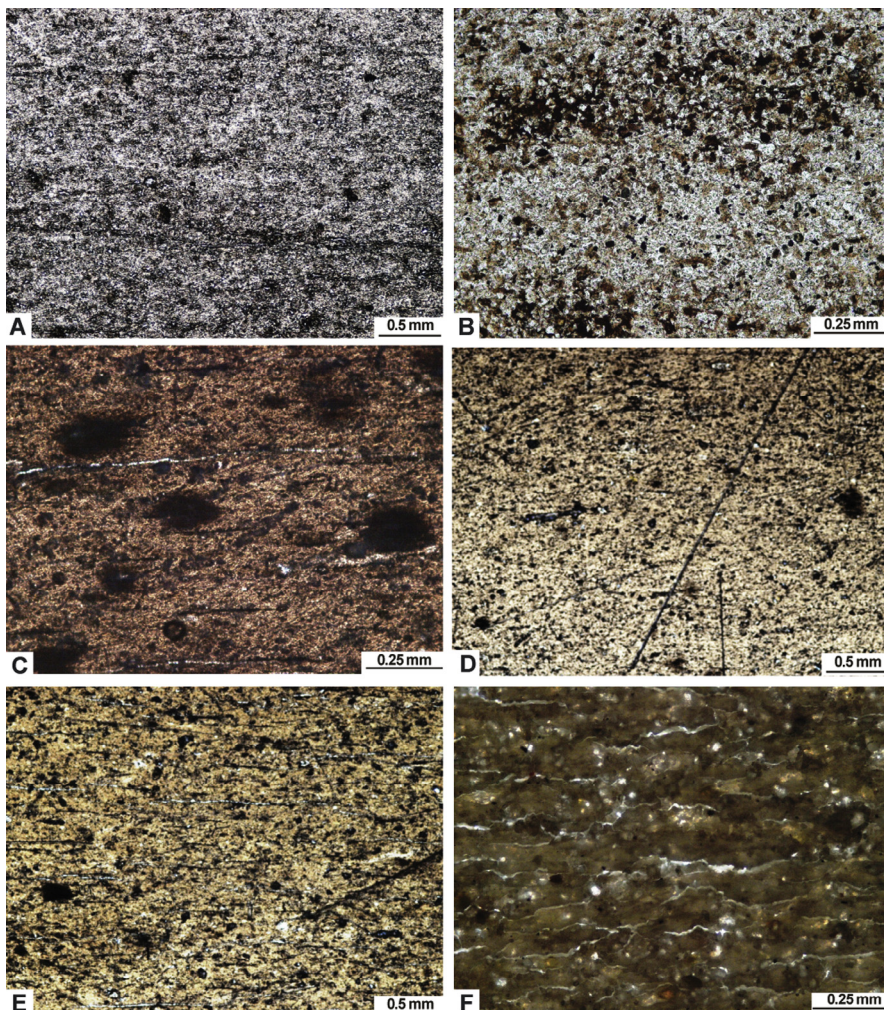


**Fig. 9 – Photomicrographs showing:** (A) Angular to subangular quartz grains in the silty claystone facies, Gebel Qarara section (GQ01), PPL. (B) Pyrite is ubiquitous in claystone microfacies. It occurs as disseminated anhedral to euhedral crystals and as irregular patches, Gebel Qarara section (GQ01), PPL. (C) Quartz and feldspars are common in discrete quartz laminae, Gebel El-Ahmar section (GA02), PPL. (D) Angular to subangular quartz grains in the silty shale microfacies, Gebel El-Ahmar section (GA06), PPL. (E) White clays, Gebel El-Ahmar section (GA02), PPL. (F) Clays are uniformly elongate parallel to laminations, Gebel El-Ahmar section (GA07), PPL.

of abundant glauconite reflects marine transgression and associated sediment starvation [16,28]. Recent studies focusing on passive-margin successions have shown that glauconite may be ubiquitous throughout a depositional sequence, but its origins (authigenic vs. detrital), abundance, and maturity vary systematically within and through systems tracts [19,29,30].

Maximum glauconite abundance and maturity are characteristics of the condensed section (CS) and the associated

surface of maximum sediment starvation, which occur at the transition between the TST and the highstand systems tract (HST). In passive-margin condensed sections, glauconite is commonly associated with concentrations of fossil debris, phosphatic grains, sulfides, carbonates horizons, and intense bioturbation [23,24,28,31,32]. In the recorded bed, fossil debris are very common with glauconite (Fig. 13B) in addition to the absence of phosphate, sulfides, and carbonates.

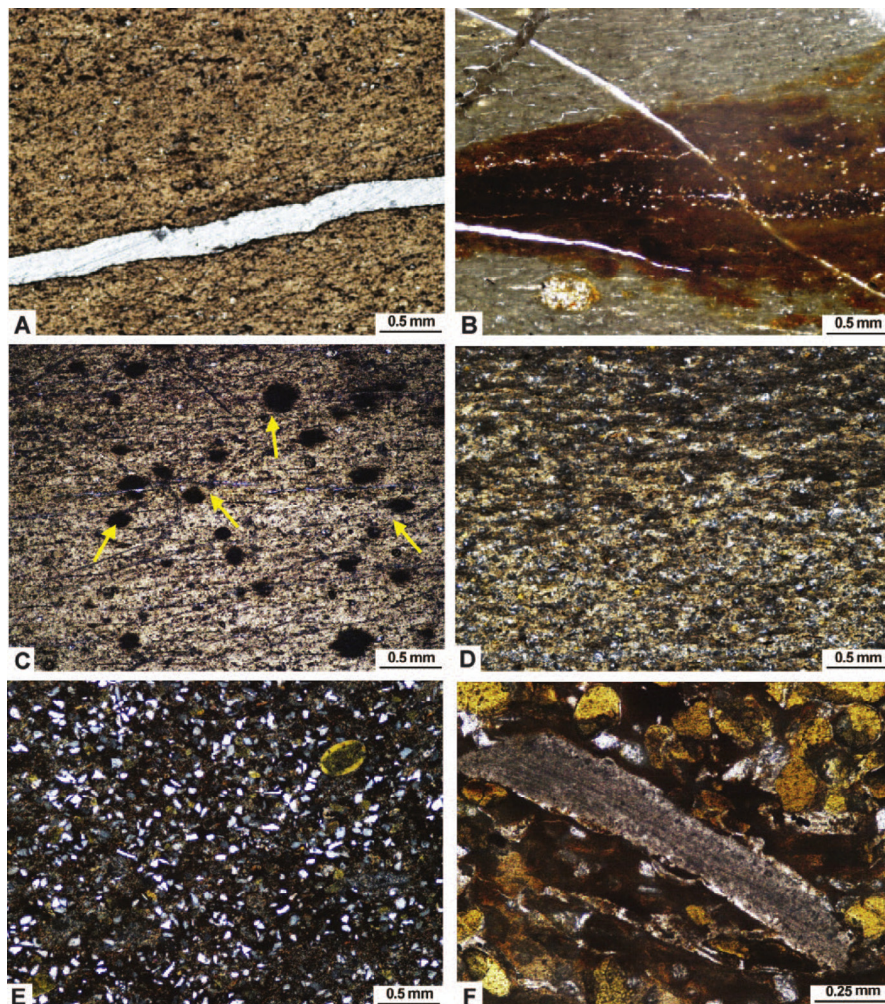


**Fig. 10 – Photomicrographs showing:** (A) Fissures in the silty shale microfacies which give fissility that later filled with gypsum, Gebel El-Ahmar section (GA06), XPL. (B) Fissures in the silty shale microfacies which give fissility that later filled with hematite, Gebel El-Ahmar section (GA07), PPL. (C) Scattered clay pellets (arrows) within silty shale with long axes parallel to lamination, Gebel El-Ahmar section (GA02), PPL. (D) Lamination in the silty shale microfacies (quartz laminae and clay laminae), Gebel El-Ahmar section (GA07), PPL; (E) Angular to subangular silt-sized quartz grains intermixed with rounded to subrounded slightly oxidized glauconite pellets, El-Sheikh Fadl section (SF06), XPL. (F) Large shell fragment, oxidized glauconite grains and few quartz grains scattered in a fine clay matrix, El-Sheikh Fadl section (SF13), PPL.

### 5.3. Depositional sequences

According to facies changes in the three studied sections, two sequences were recognized. The recorded sequences are incomplete because the base of the Qarara Formation is not exposed. These sequences range in thickness from 3 to 18 m, so they are fourth to fifth in order [33]. In Gebel Qarara section

(Fig. 5), these cycles are characterized by the presence of silty claystone at the base grading upward to silty shale facies, glauconitic fossiliferous ironstone and glauconitic bioclastic lime mudstone-wackestone facies. In El-Sheikh Fadl and Gebel El-Ahmar sections (Figs. 6 and 7), these cycles are represented by silty shale at the base, glauconitic green sand in the middle, and glauconitic bioclastic wacke-packstone at the top.

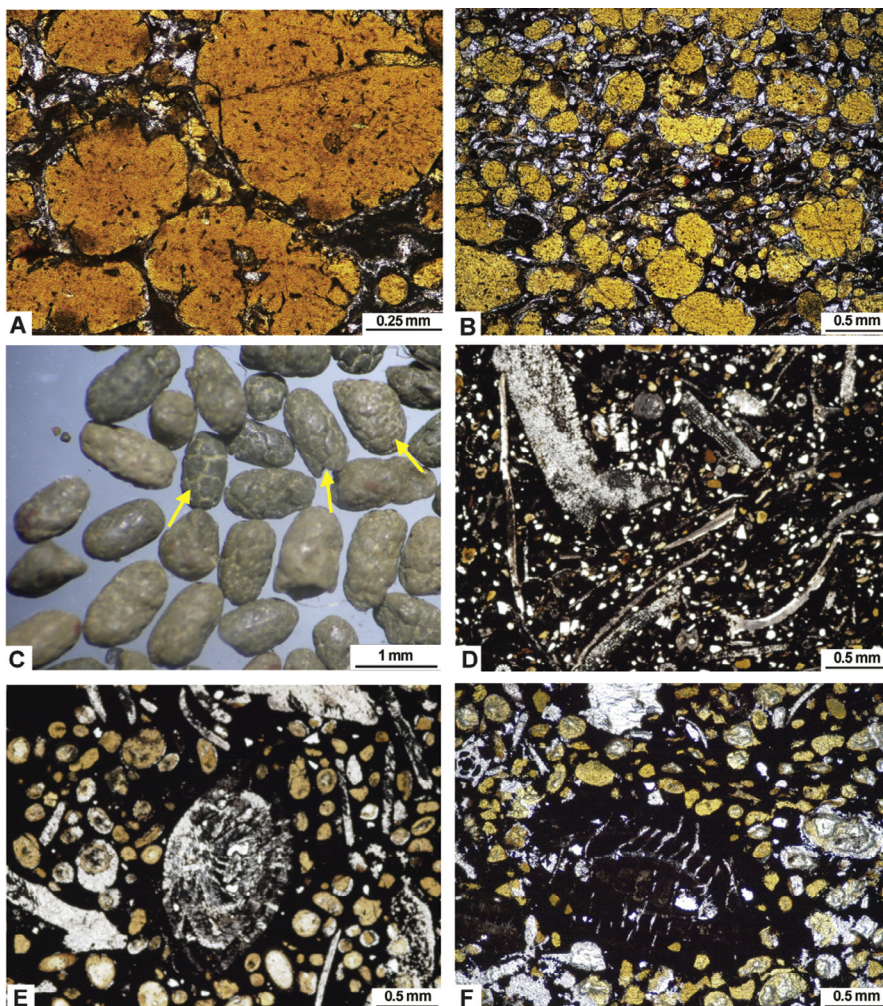


**Fig. 11 – (A)** Photomicrograph showing sand-sized, subrounded, pale green to yellow glauconite grains. Quartz grains are encountered with limited distribution. Glauconite and quartz are embedded in a glauconitic clay matrix, El-Sheikh Fadl section (SF07), PPL. **(B)** Photomicrograph showing well sorted glauconite grains, El-Sheikh Fadl section (SF07), PPL. **(C)** Glauconite grains separated from El-Sheikh Fadl section (SF07). Notice the abundance of fractured grains (arrows), whereas smooth grains are also recognized. **(D)** Photomicrograph showing echinoderms, miliolid foraminifera, gastropods, ostracods and bryozoans that embedded in a hematitic cement, Gebel El-Qarara section (GQ13), PPL. **(E)** Photomicrograph showing well rounded, well sorted glauconitic grains and large gastropod tests which are floated in a hematitic cement, El-Sheikh Fadl section (SF12), PPL. **(F)** Photomicrograph showing glauconitic fossil mold that is partially or completely replaced by iron oxides, El-Sheikh Fadl section (SF12), PPL.

From these cycles and facies changes, the deposition of the three sections has been affected by initial stages of sea level rise. The Gebel Qarara section was deposited under deeper conditions than El-Sheikh Fadl and Gebel El-Ahmar sections due to the presence of glauconitic bioclastic lime-mudstone-wackestone microfacies. This is in line with the concept of sea transgression during the Eocene period, as Gebel Qarara section lies in the north (i.e. deeper than the other two sections).

## 6. Conclusions

The Middle Eocene Qarara Formation consists of seven microfacies arranged from base to top as follows; silty claystone, silty shale, fossiliferous glauconite, glauconitic (green) sand, glauconitic fossiliferous ironstone, glauconitic bioclastic wacke-packstone, glauconitic bioclastic lime-mudstone-wackestone.

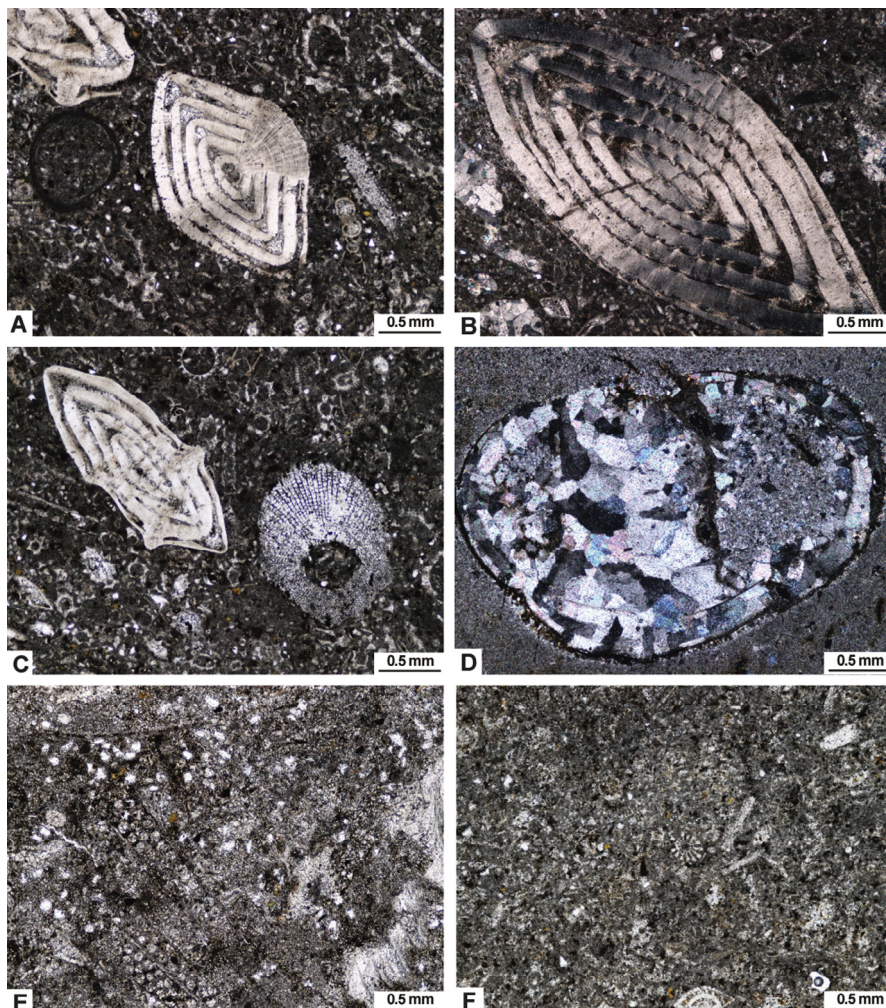


**Fig. 12 – Photomicrographs showing:** (A) Large-sized benthic nummulite foraminifera, El-Sheikh Fadl section (SF17), PPL. (B) Large-sized benthic nummulite foraminifera shows a pronounced extinction bands, El-Sheikh Fadl section (SF18), XPL. (C) Excellent preservation of nummulite foraminifera, El-Sheikh Fadl section (SF18), PPL. (D) A cavity shows geopetal-like structure, Gebel El-Qarara section (GQ16), XPL. (E) Biserial bryozoan and miliolid foraminifera embedded in a micritic matrix, Gebel El-Qarara section (GQ14), PPL. (F) Fine sand-sized grains, glauconite pellets and small nummulite, Gebel El-Qarara section (GQ14), PPL.

Shale and claystone of the studied Qarara Formation deposited in quiet water settings. The presence of glauconite represents a condensed setting in an overall calm environment. The carbonate microfacies are deposited in inner ramp setting because of presence of the larger foraminifera and bivalve fragments.

The studied rocks comprise two principal facies, lower argillaceous facies and upper carbonate one. They are separated by glauconitic fossiliferous ironstone bed. Two fourth-fifth order sequences were recognized in the

studied sections. These sequences range in thickness from 3 to 18 m.

#### Acknowledgments

The authors thank Mahmoud Lotfy and Mohamed Youssef, Department of Geology, Mansoura University, for their help during the field work. Authors would like to thank anonymous reviewers for their valuable comments.

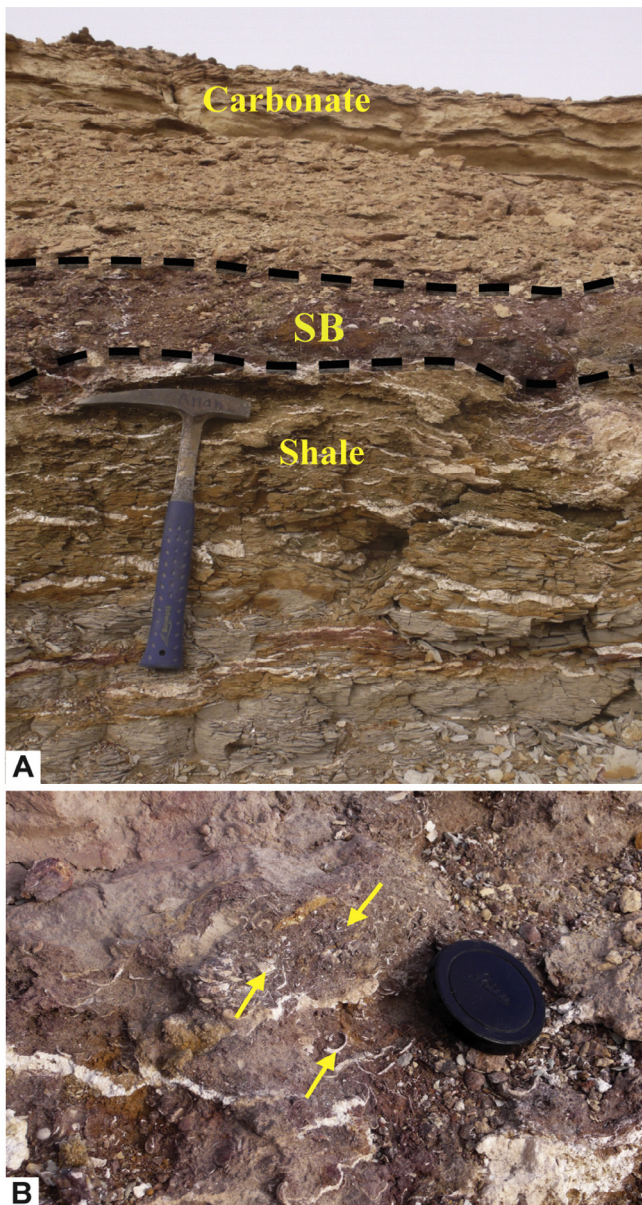


**Fig. 13 – Field photographs showing: (A)** Glauconitic fossiliferous ironstone bed which is considered as a sequence boundary (SB), geologic hammer for scale is 32.5 cm long. **(B)** Close up of glauconitic fossiliferous ironstone bed. Notice the abundance of fossil debris (arrows), lens cap for scale is 4 cm in diameter.

#### REFERENCES

- [1] Said R. Planktonic foraminifera from the Thebes Formation, Luxor, Egypt. *Micropaleontology* 1960;6:277–86.
- [2] Bishay Y. Biostratigraphic study of the Eocene in the Eastern Desert between Samalut and Assiut by the larger foraminifera. 3rd Arab Petrol Congress, Alexandria, 1961; 7 pp.
- [3] Bishay Y. Studies on the larger foraminifera of the Eocene of the Nile Valley between Assiut, Cairo and S.W. Sinai [Ph.D. thesis]. Alexandria University, Egypt; 1966.
- [4] Strougo A. Mokattamian stratigraphy of eastern Maghagha – El-Fashn district. MERC Ain Shams Univ Sci Res Ser Cairo 1986;6:33–58.
- [5] Iskander F. Geological survey of the Gharaq El Sultani sheets no 68/54. Standard Oil Co. Egypt S.A., 1943; Report no 57, 29p.
- [6] Omara S, Mansour HH, Youssef M, Khalifa H. Stratigraphy, paleoenvironment and structural features of the area east of Beni Mazar, Upper Egypt. *Bull Fac Sci Assiut Univ* 1977;6(3):171–97.
- [7] Cronin TM, Khalifa H. Middle and late Eocene Ostracoda from Gebel El Mereir, Nile Valley, Egypt. *Micropaleontology* 1979;25(4):397–411.
- [8] Hermina M, Lindenberg H. The tertiary. In: Hermina M, Klitzsch E, List FK, editors. (1989) *Stratigraphic lexicon and explanatory notes to the geological map of Egypt*. Cairo: Conoco Inc.; 1979 1:500000.
- [9] Dunham RJ. Classification of carbonate rocks according to depositional texture. In: Ham WE, editor. *Classification of carbonate rocks*, vol. 1. American Association of Petroleum Geologists Memoir; 1961. p. 108–21.
- [10] Hardy R, Tucker M. X-ray powder diffraction of sediments. In: Tucker M, editor. *Techniques in sedimentology*. Blackwell Scientific Publications; 1988. p. 191–228.
- [11] Folk RL. Petrology of sedimentary rocks. Hempill's: Austin; 1968.
- [12] Picard MD. Classification of fine-grained sedimentary rocks. *J Sediment Petrol* 1971;41:179–95.
- [13] Pettijohn FJ. *Sedimentary rocks*. 2nd ed. New York: Harper and Row; 1957.
- [14] Schieber J, Southard J, Thaisen K. Accretion of mudstone beds from migrating floccule ripples. *Science* 2007;318:1760–3.
- [15] Odin GS, Fullagar PD. Geological significance of the Glaucony Facies. In: Odin GS, editor. *Green marine clay*. Amsterdam: Elsevier; 1988. p. 295–332.
- [16] Amorosi A. Detecting compositional, spatial, and temporal attributes of glaucony: a tool for provenance research. *Sediment Geol* 1997;109:135–53.
- [17] Heckel PH. Recognition of ancient shallow marine environments. In: Rigby JK, Hamblin WK, editors. *Recognition of ancient sedimentary environments*, vol. 16. SEPM Special Publication; 1972. p. 226–86.
- [18] McRae SG. Glauconites. *Earth Sci Rev* 1972;8:397–440.
- [19] Huggett JM, Gale AS. Petrology and paleoenvironmental significance of glaucony in the Eocene succession at Whitecliff Bay, Hampshire Basin, UK. *J Geol Soc Lond* 1997;154:897–912.
- [20] Scholle PA, Ulmer-Scholle DS. A color guide to the petrography of carbonate rocks: grains, textures, porosity, diagenesis. AAPG Memoir; 2007. p. 77.
- [21] Wilson JL. *Carbonate facies in geologic history*. New York, Heidelberg, Berlin: Springer-Verlag; 1975.
- [22] Flügel E. *Microfacies of carbonate rocks: analysis, interpretation and application*. 2nd ed. Berlin: Springer-Verlag; 2010.
- [23] Amorosi A. Glaucony and sequence stratigraphy: a conceptual framework of distribution in siliciclastic sequences. *J Sediment Res* 1995;B65:419–25.
- [24] Kitamura A. Glaucony and carbonate grains as indicators of the condensed section: Omma Formation, Japan. *Sediment Geol* 1998;122:151–63.
- [25] Catuneanu O. *Principles of sequence stratigraphy*. Amsterdam: Elsevier; 2006.
- [26] Galloway WE. Genetic stratigraphic sequences in basin analysis. I. Architecture and genesis of flooding-surface bounded depositional units. *Am Assoc Pet Geol Bull* 1989;73:125–42.

- [27] Brown LF Jr, Fisher WL. Seismic stratigraphic interpretation of depositional systems: examples from Brazilian rift and pull-apart basins. In: Payton CE, editor. *Seismic stratigraphy—applications to hydrocarbon exploration*, vol. 26. American Association of Petroleum Geologists Memoir; 1979. p. 213–48.
- [28] Baum GR, Vail PR. Sequence stratigraphic concepts applied to Paleogene outcrops, Gulf and Atlantic basins. In: Wilgus CK, Hastings BS, Ross CA, Posamentier HW, Van Wagoner J, Kendall CG, editors. *Sea-level changes: an integrated approach*, vol. 42. Society of Economic Paleontologists and Mineralogists, Special Publication; 1988. p. 309–27.
- [29] Harris LC, Whiting BM. Sequence-stratigraphic significance of Miocene to Pliocene glauconite-rich layers, on- and offshore of the US Mid-Atlantic margin. *Sediment Geol* 2000;134:129–47.
- [30] Hesselbo SP, Huggett JM. Glaucony in ocean-margin sequence stratigraphy (Oligocene-Pliocene, offshore New Jersey, U.S.A.; ODP Leg 174A). *J Sediment Res* 2001;71:599–607.
- [31] Pemberton SG, Maceachern JA, Frey RW. Trace fossils facies models: environmental and allostratigraphic significance. In: Walker RG, James NP, editors. *Facies models response to sea level change*. Geological Association Canada; 1992. p. 47–72.
- [32] Urash RG II. *Sedimentology and ichnology of a passive margin condensed section, Eocene Lisbon Formation, Southern Alabama [Unpublished MS thesis]*. Auburn University; 2005.
- [33] Vail PR, Mitchum RM Jr, Thompson S III. *Seismic stratigraphy and global changes of sea level, Part four: global cycles of relative changes of sea level*, vol. 26. American Association of Petroleum Geologists Memoir; 1977. p. 83–98.
- [34] Bassiouni MA, Boukhary MA, Anan HS. Ostracodes from Gebel Gurnah, Nile Valley, Egypt. *Proc Egyptian Acad Sci* 1977;30:1–9.